JOURNAL OF MATERIALS SCIENCE 27 (1992) 1469–1474

Structure and mechanical properties of brittle starch foams

S. C. WARBURTON, A. M. DONALD
Cavendish Laboratory, Madingley Road, Cambridge, UK
A. C. SMITH
AFRC Institute of Food Research, Colney Lane, Norwich, UK

The mechanical properties of extrusion-cooked maize have been analysed according to the Gibson and Ashby models of closed cell foams. The data point to better agreement with the earlier model and indicate that the cell-face bending term is not negligible for foams with little draining into the cell edges. The shape of the cells in these maize foams changes with foaming conditions: non-equilibrium spherical cells with some anisotropy are formed at conditions of low moisture content or high temperature when the glass transition temperature, T_g, is elevated. Polyhedral cells which show some draining of material into the cell edges are formed under the converse conditions when the T_g is lower. The change from polyhedral to spherical cells is also accompanied by a change in amylose–lipid complex from the V to the metastable E type, as shown by X-ray diffraction.

1. Introduction

The understanding of the mechanical properties of solid foams has been enhanced and consolidated in recent years by the work of Ashby and Gibson [1–3]. The original treatment [2] considered idealized closed and open cell foams deforming elastically, plastically and by fracture. The generalized equation took the form

$$\frac{\sigma}{\sigma_w} = C\left(\frac{\rho}{\rho_w}\right)^n \quad (1)$$

where σ is the mechanical property, ρ is the density of the foam, C is a constant, and the subscripted quantities refer to the foam walls. The value of n varied with the deformation mode and connectivity of the foam. When σ is the Young's modulus, $n = 3$ for closed cell and $n = 2$ for open cell foams. When σ is the fracture strength, $n = 2$ for closed cell and $n = 1.5$ for open cell foams. Ashby [2] provided evidence that the response of foamed polymers, ceramics and metals obeyed this equation. In these cases, σ_w was identified with the mechanical property of the bulk material. The Ashby treatment also provides an elegant framework for the description of food foams, although in this case the value of σ_w cannot simply be identified with a bulk value because the reactive nature of food processing prevents the unexpanded food from being representative of the foam walls [4].

Baer [5] indicated a simple power-law relationship between mechanical properties and density for synthetic polymer foams

$$\sigma \propto \rho^n \quad (2)$$

Equation 2 is a special case of Equation 1 for a constant value of σ_w/ρ_w^n. Studies with extrusion-cooked foams originally tested Equation 2 in a number of stress states and found good agreement [6]. In all cases the values of n were higher for stiffness than strength, as predicted by Ashby, although the values of n were more consistent with the open cell predictions despite the foams being clearly of the closed cell type. Ashby pointed to the fact that closed cell foams often have the material concentrated in the cell walls leading to open cell type behaviour although the available evidence suggests that there is no particular concentration of material for the extrudates.

More recently, direct measurements were made of the wall mechanical properties allowing explicit testing of Equation 1 [7]. Although there was a negligible change in wall mechanical properties over the bulk density range considered, there was a significant variation in the wall density. The quantitative fitting of Equation 1 showed values of n in agreement with the closed cell prediction for strength and in excess of the prediction for modulus.

Recent developments of the foam model [3] have incorporated different contributions to the deformation of closed cell foams. The Young's modulus is the sum of three contributions in the absence of cell fluid. The first is cell-edge bending which gives a contribution of the same form as for open cell foams although it depends on the fraction, ϕ, of solid contained in the cell edges. The second contribution is due to membrane stresses in the cell faces as the cell edges bend. Finally, a contribution due to cell-face bending follows the form of the original closed cell power law, albeit modified by the amount of material in the cell face.

0022–2461

TABLE I Cell shape as a function of extrusion temperature and water content; P = polyhedral, S = spherical and ? = intermediate

Extrusion temperature (°C)	Water content (% wet weight basis (w.w.b.))										
	10.9	13.4	15.8	18.0	20.2	22.2	24.1	26.0	27.7	29.4	31.0
80	S	S	?	P							
100	S	S	?	P							
120	S	S	?	P	P	P					
140		S	S	?	P	P	P				
160			S	?	P	P	P	P	P		
180		S	S	?	P	P	P	P	P	P	P
200		S	S	?	P	P	P	P	P		

The resulting equation is

$$\frac{E}{E_w} = C_1\phi^2\left(\frac{\rho}{\rho_w}\right)^2 + C_2(1-\phi)\left(\frac{\rho}{\rho_w}\right) + C_3(1-\phi)^3\left(\frac{\rho}{\rho_w}\right)^3 \quad (3)$$

compared with $n = 3$ in Equation 1 in the original treatment.

By analogy, the equation for the brittle fracture stress of closed cell foams is

$$\frac{\sigma}{\sigma_w} = C_1'\phi^{3/2}\left(\frac{\rho}{\rho_w}\right)^{3/2} + C_2'(1-\phi)\left(\frac{\rho}{\rho_w}\right) + C_3'(1-\phi)^2\left(\frac{\rho}{\rho_w}\right)^2 \quad (4)$$

which compares with $n = 2$ in Equation 1 according to the earlier model. Gibson and Ashby [3] pointed out that the cube-power term in Equation 3 was vanishingly small which leads to a reduced overall power of the normalized density compared to Equation 1. The experimental evidence from a wide range of foams using the approximate relationship of Equation 2 [6] points to better agreement with the lower power-law predictions of Equations 3 and 4 in comparison with Equation 1. In contrast, the recent experimental evaluation of Equation 1 [7] for maize foams shows that Equations 3 and 4 underpredict the observed power laws and that the earlier model (Equation 1) gives a better description of the data.

This paper describes an assessment of the experimental data on the structure and mechanical properties of extrusion-cooked maize foams in the light of the latest model, and also discusses the origins of the foam structure in terms of the foam solidification step of the extrusion-cooking process.

2. Experimental procedure

The samples were produced from maize grits using a Baker Perkins MPF 50D co-rotating twin-screw extruder. The full details of the experimental conditions have been given previously [7]. Cylindrical specimens were produced which were dried at 40 °C and stored.

The foam cylinders were cut perpendicular and parallel to their axes and gold-plated prior to performing scanning electron microscopy (SEM). The scanning electron micrographs were examined to obtain the average cell size and cell-wall thickness of 50 cells. The shape of the cells was also recorded. The anisotropy of the cell size was investigated by measuring the three perpendicular intercept lengths from the micrographs as defined in Fig. 1. These lengths were derived from the reciprocal of the number of intercepts per unit length for 100 foam cells.

Differential scanning calorimetry (DSC) was used to determine the glass transition temperature, T_g, as described earlier. A Mettler TA3000 system was used to analyse foam samples that had been ground after extrusion [7].

X-ray diffraction (XRD) studies were achieved with ground, dried extrudate mounted in glass capillaries using a Debye–Scherrer camera. The location of the diffraction peaks corresponding to amylose–lipid complexes was measured.

3. Results

Scanning electron micrographs of the foams show that they are clearly of the closed cell type (Fig. 2) and are polyhedral or spherical in shape. The polyhedral cells show some "draining" of material from the cell faces into the edges, whereas this is negligible for the spherical-shaped cells (see also Fig. 6 in [7]). Table I shows the gradual transition from polyhedral to spherical cells with increasing extrusion temperature and decreasing water content. Table II summarizes the occurrence of the E and V type amylose–lipid diffraction peaks for the same extrusion conditions as shown in Table I. With increasing extrusion temperature and decreasing water content, there is a gradual introduction of the E type complex.

Tables III and IV show the structural characteristics of the different foams. It includes values of the volume fraction of material in the cell edges, ϕ, defined

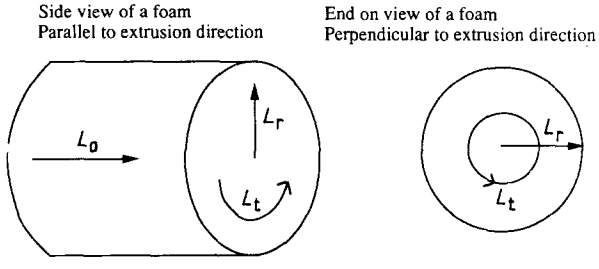

Figure 1 Anisotropy of the foam cells, defining the axial, radial and tangential intercept lengths.

TABLE II Type of amylose–lipid complex as a function of extrusion temperature and water content, as determined by X-ray diffraction. strong peak, w, weak peak

Extrusion temperature (°C)	Water content (% w.w.b.)										
	10.9	13.4	15.8	18.0	20.2	22.2	24.1	26.0	27.7	29.4	31.0
80	Eh (s) Vh (w)	Eh (s) Vh (w)	Vh (s) Eh (w)	Vh							
100	Eh (s) Vh (w)	Eh (s) Vh (w)	Vh (s) Eh (w)	Vh							
120	Eh (s) Vh (w)	Eh (s) Vh (w)	Vh (s) Eh (w)	Vh	Vh	Vh					
140		Eh (s) Vh (w)	Vh (s) Eh (w)	Vh (s) Eh (w)	Vh	Vh	Vh				
160			Eh (s) Vh (w)	Vh (s) Eh (w)	Vh	Vh	Vh	Vh	Vh		
180		Eh (s) Vh (w)	Eh (s) Vh (w)	Vh (s) Eh (w)	Vh (s) Eh (w)	Vh	Vh	Vh	Vh	Vh	Vh
200		Eh (s) Vh (w)	Eh (s) Vh (w)	Vh (s) Eh (w)	Vh (s) Eh (w)	Vh	Vh	Vh	Vh		

as [3]

$$\phi = \frac{t_e^2}{t_e^2 + Z_f t_f l/\langle n \rangle}$$

where l is the cell size, $\langle n \rangle$ is the mean number of edges per face, t_e is the cell-edge thickness, t_f is the cell-face thickness and Z_f is the face connectivity or the number of faces that meet at an edge. $Z_f = 3$ for the foams produced in this study and $\langle n \rangle$ was assumed to be 5 [8].

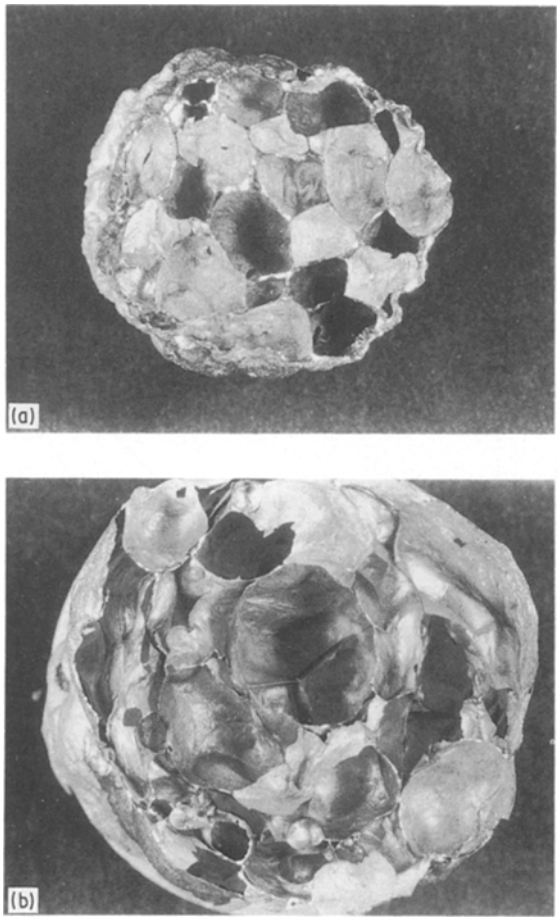

Figure 2 Optical micrographs of foams sectioned diametrically showing (a) polyhedral, and (b) spherical-shaped cells.

Tables V and VI list the anisotropy factors for the foams. Values of L_r were consistently lower than those of L_a and L_t.

4. Discussion

The observed values of ϕ (Tables III and IV) show that $\phi \sim 0.5$ for polyhedral cells and $\phi \sim 0.1$ for spherical cells. It follows from Equations 3 and 4 that the relationship between mechanical properties and density is predicted to show a change of slope when the cell shape changes. Figs 3 and 4 show the data from [7] with the model predictions for $\phi = 0, 0.5$ and 1. The constants were set at $C_1 = C_2 = C_2' = 1$ and $C_1' = 0.65$ as described in [3]. The contributions of face bending were ignored as suggested by Gibson and Ashby [3], i.e. $C_3 = C_3' = 0$ in Equations 3 and 4. The experimental results do not confirm these predictions of the model.

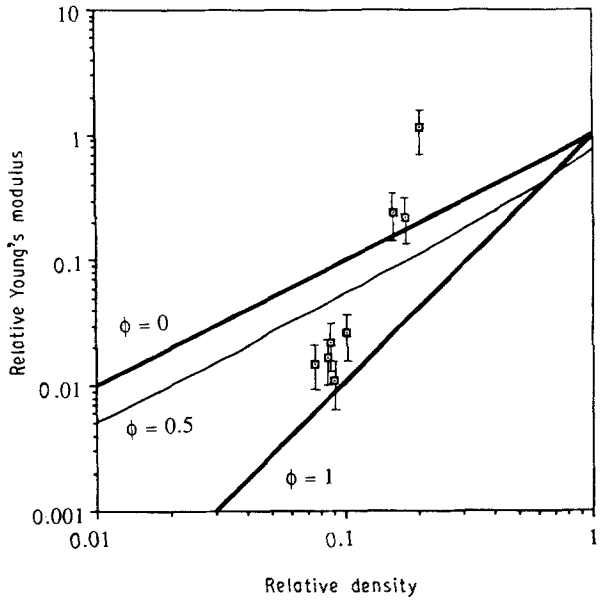

Figure 3 Relative Young's modulus of the foams as a function of relative density, plotted logarithmically. The predictions using Equations 3 and 4 for different values of ϕ are also shown.

TABLE III Variation of foam characteristics with extrusion temperature at a water content of 15.8% w.w.b. X = indeterminate, S = spherical and P = polyhedral. Figures in brackets indicate standard deviations

Extrusion temperature (°C)	Density (g cm^{-3})	Mean cell size (mm)	Mean wall thickness (μm)	Estimate of ϕ	Cell shape
80	0.27	2.1 (1.3)	90 (80)	0.3	X
100	0.24	2.3 (1.3)	75 (60)	0.2	X
120	0.16	3.9 (2.3)	100 (65)	0.1	X
140	0.12	3.5 (2.1)	55 (35)	0.03	S
160	0.10	3.0 (2.3)	100 (65)	0.03	S
180	0.11	3.4 (2.4)	45 (30)	0.02	S
200	0.12	3.0 (2.4)	45 (25)	0.02	S

TABLE IV Variation of foam characteristics with water content during extrusion at an extrusion temperature of 160 °C. X = indeterminate, S = spherical and P = polyhedral. Figures in brackets indicate standard deviations

Extrusion water content (% w.w.b.)	Density (g cm^{-3})	Mean cell size (mm)	Mean wall thickness (μm)	Estimate of ϕ	Cell shape
27.7	0.37	1.7 (1.4)	160 (120)	0.6	P
26.0	0.34	1.8 (1.1)	160 (140)	0.4	P
24.1	0.33	2.1 (1.2)	170 (140)	0.4	P
22.2	0.32	2.2 (1.3)	150 (130)	0.3	P
20.2	0.19	2.3 (1.6)	100 (60)	0.1	P
18.0	0.18	2.9 (1.9)	110 (90)	0.1	X
15.8	0.10	3.0 (2.3)	60 (40)	0.03	S

TABLE V Variation of mean intercept lengths (defined in Fig. 1) with extrusion temperature at a water content of 15.8% w.w.b. during extrusion, and the ratios L_a/L_t and L_t/L_r

Extrusion temperature (°C)	L_r (mm)	L_a (mm)	L_t (mm)	L_a/L_t	L_t/L_r
80	1.4	1.7	1.7	1.2	1.2
100	1.5	1.7	1.9	1.1	1.3
120	2.5	2.6	3.2	1.0	1.3
140	2.1	2.7	2.6	1.3	1.2
160	2.0	2.5	2.8	1.3	1.4
180	2.0	2.8	2.7	1.4	1.4
200	1.9	2.2	2.8	1.2	1.5

TABLE VI Variation of mean intercept lengths (defined in Fig. 1) with water content during extrusion at a temperature of 160 °C, and the ratios L_a/L_t and L_t/L_r

Extrusion water content (% w.w.b.)	L_r (mm)	L_a (mm)	L_t (mm)	L_a/L_t	L_t/L_r
27.7	1.2	1.7	1.4	1.4	1.2
26.0	1.4	1.8	1.6	1.3	1.1
24.1	1.4	2.3	1.9	1.6	1.4
22.2	1.5	2.2	1.8	1.5	1.2
20.2	1.6	2.6	2.2	1.6	1.4
18.0	1.7	2.3	2.4	1.4	1.4
15.8	2.0	2.5	2.8	1.3	1.4

It is noteworthy that the argument used for the negligible contribution of the highest power term in Equations 3 and 4 is that ϕ tends to 1 and that ρ/ρ_w is small. The values of ϕ indicate that the face-bending contribution may not be negligible for these foams particularly at low densities. Furthermore the values of C_3 and C'_3 are not known for these materials but the fitting of Equation 1 to the data of Figs 3 and 4 indicate that $C \sim 100$. On the basis of Equation 1 arising from cell-face bending, C may be identified with C_3 and C'_3. The net effect is that although the cell-wall bending contribution is described as being small in Equations 3 and 4, this will not be the case if the values of C_3, and C'_3 are large and if $\phi \ll 1$. This may rationalize why these maize foams obey the

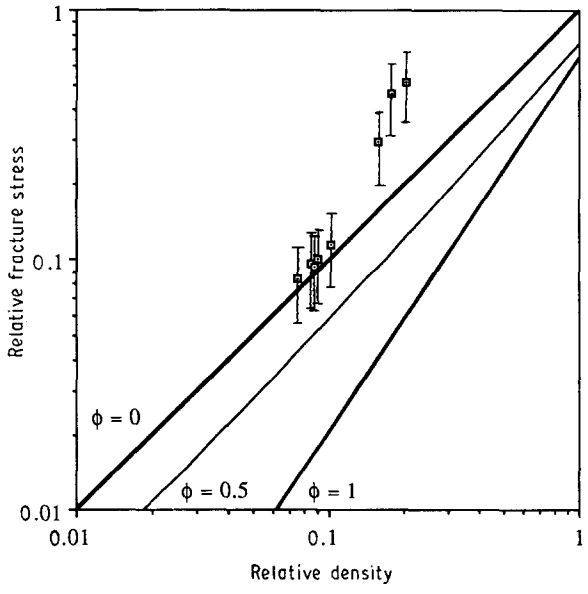

Figure 4 Relative fracture stress of the foams as a function of relative density, plotted logarithmically. The predictions using Equations 3 and 4 for different values of ϕ are also shown.

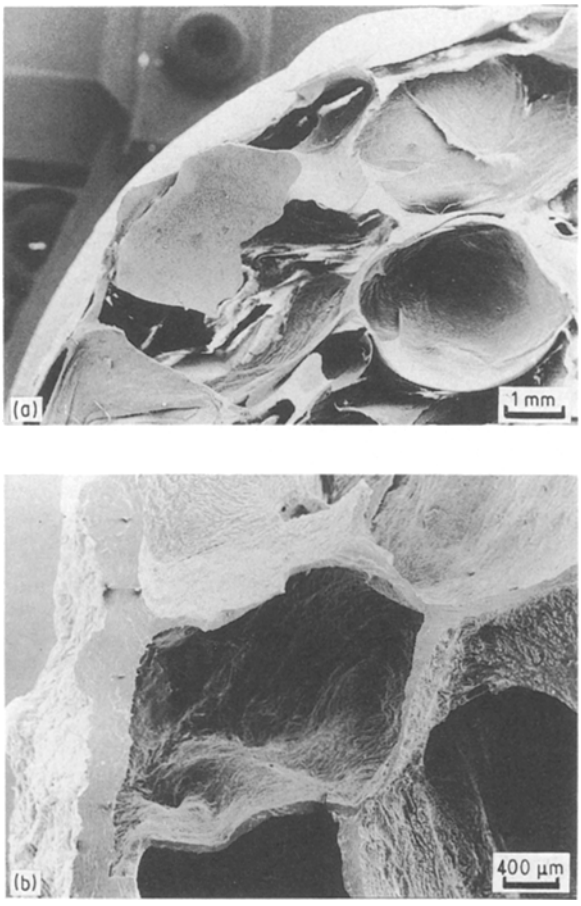

Figure 5 Optical micrographs of (a) spherical- and (b) polyhedral-shaped cells showing the thicker outer walls for the polyhedral cells.

earlier predictions of Ashby and Gibson rather than the later ones.

Other reasons for the high value of the power law to describe the data of Fig. 3 and 4 can also be put forward. It might arise from the formation of a sandwich structure at high densities (Fig. 5). The foam cylinder appears to develop a thicker outer wall at high densities causing a reinforcing effect where the stress is borne by the unfoamed annular cross-section surrounding the foam. Another possible contribution is the anisotropy of the foam cells which is known to affect mechanical properties. The cell shapes are not precisely isotropic (Tables V and VI). The anisotropy of the foams cells between the axial and radial directions, L_a/L_r, indicates that the polyhedral cells are more elongated in the extrusion direction than the spherical cells. The ratio L_t/L_r indicates the restriction of cell growth near the surface of the foam which would tend to squeeze cells in the radial direction and elongate them in the tangential direction. Solidification of the surface layer will occur faster under conditions of high temperature and low water content. These are also the conditions for spherical cells, which are therefore more distorted perpendicular to the extrusion direction than the polyhedral cells. It was noted that the modulus results deviate more from the model than the strength results ([7]; Figs 3 and 4) which is consistent with the report of Huber and Gibson [9] that the shape anisotropy has a greater effect on stiffness than strength.

Rubens [10] reported a treatment of synthetic foam formation in which foam growth depends on the glass transition temperature and the amount of blowing agent. If foams are extruded at high temperatures then all the gas is evolved before solidification. The degree of expansion then depends on the blowing agent content. However, collapse of the foam occurs on cooling as the gas contracts prior to solidification. Extrusion at a lower temperature leads to solidification before the release of all the gas and hence expansion is temperature dependent. This points to a minimum density depending on the glass transition and the blowing agent solubility in the polymer melt. These arguments do not carry over exactly to the extrusion-cooking process because the water content may not be treated simply as a conventional blowing agent. Fig. 6 shows the variation of density with moisture content for different extrusion temperatures. The increase in density with increasing moisture content shows that water is not simply acting as a blowing agent. An increase in water content reduces the viscosity which enhances bubble growth, but simultaneously the reduced die pressure reduces the expansion force. The evidence suggests the latter effect dominates.

The effect of water is not merely to control the amount of expansion possible because it also affects T_g which controls the arrest of bubble growth. The variation of T_g with extrusion moisture is shown in Fig. 7 and comprises the data obtained on the extruded material after water has been lost during the foaming process. The predictions of T_g for starch as a function of moisture content are also shown [11]. Material leaving the extruder is above the glass transition but as it loses moisture two changes take place; the T_g increases and at the same time the material cools. A high initial moisture content or low extrusion temperature means there is a comparatively long time before the material passes through the T_g. This means there is time for equilibrium to be reached and as the loss of moisture proceeds and the temperature drops, the driving force for expansion will also be reduced. There

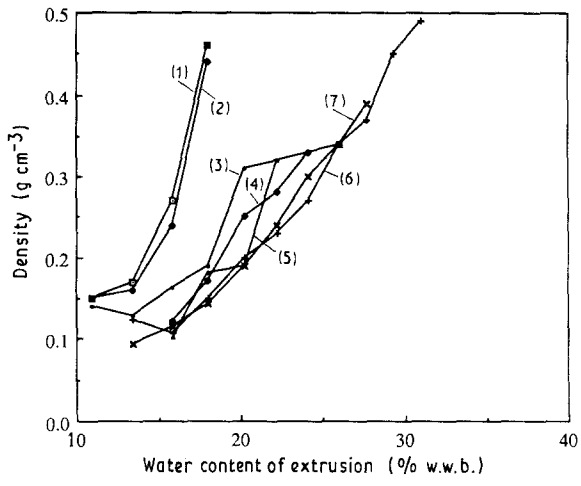

Figure 6 The bulk density of the foams as a function of extrusion water content at (1) 80 °C, (2) 100 °C, (3) 120 °C, (4) 140 °C, (5) 160 °C, (6) 180 °C, (7) 200 °C.

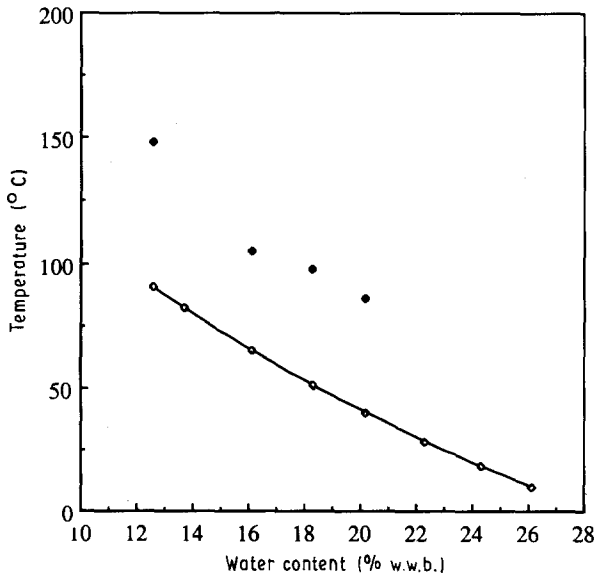

Figure 7 The observed (◆) T_g values as a function of extrusion water content and calculated (◇) values for starch from [11].

is time for some drawing of material into the cell edges which is consistent with values of $\phi \gg 0$. On the other hand, at the extreme of very low moisture, expansion is rapid. In general it seems that a low moisture content leads to T_g being sufficiently high that the extrudate cools through it before the process of bubble growth is complete, this being more likely if the available water is limited. When T_g is above 100 °C the cells change shape to non-equilibrium spheres with a low level of draining of material from the cell faces to their edges, resulting in very low values of ϕ. It is interesting that spherical cells occur in the low-density foams indicating that they are not a consequence of non-impingement of bubbles.

A comparison of Tables I and II shows the correspondence between the occurrence of polyhedral-shaped cells and the V type amylose–lipid complex. The E type amylose–lipid complex features strongly in the material comprising the spherical-shaped cells. The E type complex represents a non-equilibrium molecular structure which is transformed into the V type complex on conditioning at higher moisture contents [12]. The same short-term extrusion processes also produce the large-scale non-equilibrium spherical foam structure.

5. Conclusions

The Young's modulus and fracture stress of extrusion-cooked maize foams have been analysed according to the Gibson and Ashby models of closed cell foams. The data point to better agreement with the simpler, earlier model based on face bending alone. Although Gibson and Ashby's later model indicates that the cell-face bending term is negligible compared with edge bending and face shrinkage, the present results for foams with little draining into the cell edges suggest that the face-bending contribution cannot be ignored and indeed seems to dominate.

The variation of the glass transition temperature with foaming conditions influences the shape of the foam cells. Low-density foams incorporating spherical cells with some anisotropy between the centre and the surface of a foamed cylinder were formed at conditions of low moisture content or high temperature. This corresponds to elevation of the glass transition temperature, T_g, and a reduction in the time scale of foaming. There was negligible draining of material to the cell edges for these foams. Polyhedral cells occurred in the higher density foams which showed some draining of material into the cell edges and were formed under conditions of high processing moisture or low temperature when the T_g is lower and the foaming time-scale longer.

Shortening the time-scale of foaming is not only accompanied by a change in cell shape from polyhedral to spherical, but also in the amylose–lipid complex from the V to the metastable E type.

Acknowledgements

The authors thank Professor M. F. Ashby, FRS, for fruitful discussions and the SERC and AFRC for financial support.

References

1. L. J. GIBSON and M. F. ASHBY, *Proc. Soc. A* **382** (1982) 25.
2. M. F. ASHBY, *Metall. Trans. A* **14** (1983) 1755.
3. L. J. GIBSON and M. F. ASHBY, "Cellular Solids: Structure and Properties" (Pergamon Press, Oxford, 1988).
4. J. M. HARPER, "Extrusion of Foods" (CRC Press, Boca Raton, 1981).
5. E. BAER, "Engineering Design for Plastics" (Chapman and Hall, New York, 1964).
6. R. J. HUTCHINSON, G. D. E. SIODLAK and A. C. SMITH, *J. Mater. Sci.* **22** (1987) 3956.
7. S. C. WARBURTON, A. M. DONALD and A. C. SMITH, *ibid.* **25** (1990) 4001.
8. D. WEAIRE and N. RIVIER, *Contemp. Phys.* **25** (1984) 59.
9. A. T. HUBER and L. J. GIBSON, *J. Mater. Sci.* **23** (1988) 3031.
10. L. C. RUBENS, *J. Polym. Sci. C. Symp.* **72** (1985) 241.
11. P. D. ORFORD, R. PARKER, S. G. RING and A. C. SMITH, *Int. J. Biol. Macromol.* **11** (1989) 91.
12. C. MERCIER, R. CHARBONNIERE, D. GALLANT and A. GUILBOT, in "Polysaccharides in Food", edited by J.M.V. Blanshard and J. R. Mitchell (Butterworths, London, 1979) p. 153.

Received 17 October 1990
and accepted 25 March 1991